

# My Title

Si Xie and Pekka K. Sinervo  
*University of Toronto*

3 September 2004

## Abstract

We study the effects of QCD interactions between the bottom quark jet and the rest of the event in top quark decays. These are dominated in Monte Carlo models by the colour effects linking the initial state hard scattering process with the final state  $b$  quark and the resulting fragmentation. We compare HERWIG and PYTHIA calculations and find that these colour effects are of the order of 3% of the overall energy seen in a  $b$  quark jet cone of radius  $R = 0.4$ , and that variations in cluster fragmentation or string fragmentation models result in systematic uncertainties in these effects of the order of 1% of the  $b$  jet energy scale.

## 1 Introduction

In current top quark mass measurements, the emphasis is shifting increasingly towards reducing systematic uncertainties. This trend will continue as more data is accumulated and the statistical uncertainties shrink further. It is an established fact that the dominating contribution to the systematic uncertainty is the jet energy scale. Consequently, understanding some of the specific effects contributing to the jet energy scale is essential for future top quark mass measurements.

In this study, we identify the contribution of colour flow interactions on the uncertainties in the  $b$  jet energy scale in  $t\bar{t}$  events. We also explore the differences of this effect as a result of various hadronization models and their respective parameters. This is done mainly by comparing different Monte Carlo samples generated by HERWIG and PYTHIA and tuning a number of relevant parameters.

Specifically, we study  $t\bar{t}$  events generated from  $\bar{p}p$  collisions. Generically, a top quark will decay into a  $W$  boson and a  $b$  quark. The  $W$  will decay into a  $q\bar{q}$  pair (hadronic channel) or a lepton and a neutrino (leptonic channel). The quarks will then subsequently fragment resulting in parton showers that are identified in the detector as jets. Since the top quark is actually coloured, a colour connection exists between the initial partons which form the  $p$  or  $\bar{p}$  beam and the  $b$  quark. Thus we expect that there be some colour interactions between partons of the initial beam and partons produced by fragmentation of the  $b$  quark. Additionally, initial state radiation and final state radiation will complicate the situation. It is also clear that this process is deeply influenced by the actual fragmentation mechanism.

The process by which a high energy parton fragments into a shower of observable final state hadrons is generically called hadronization. Unfortunately, this process is inherently non-perturbative in nature and thus cannot be described simply by QCD calculations alone. This produces the need for various phenomenological models to describe this very important process in high energy physics. Among these, two models in particular have emerged as most successful: the Cluster Hadronization Model and the Lund String Model. They are employed in the HERWIG and PYTHIA Monte Carlo generation programs, respectively. We will attempt to summarize their respective fragmentation mechanisms in the following subsections.

## 1.1 Cluster Hadronization

The Cluster Hadronization model is based on the idea that colour connected quarks can be joined into a single cluster entity and then decay according to the properties of the cluster. It reduces the complicated process of forming colourless hadrons from numerous quarks into a comparatively simpler process of forming a pair of hadrons from the single cluster.

In the first stage of hadronization, all radiated gluons will split into qqbar pairs resulting in a parton shower. Subsequently, any colour connected partons are combined pairwise into clusters. A cluster will then decay in a number of ways depending on its mass. There is a specific mass threshold above which the cluster must “split.” This threshold,  $M_{max}$ , is given by a formula involving the two relevant model parameters CLMAX and CLPOW and the constituent quark masses:

$$Mass_{max}^{CLPOW} = CLMAX^{CLPOW} + (m_1 + m_2)^{CLPOW}. \quad (1)$$

If the cluster mass is above this threshold, then the cluster must fission iteratively by introducing a qqbar pair and combining them pairwise with the original two partons of the cluster. The flavour is chosen randomly from  $u, d$ , or  $s$ . This process must continue until all clusters are below the mass threshold.

Otherwise, the cluster will decay isotropically into two colourless hadrons formed by combining a  $q\bar{q}$  pair from the vacuum and combining them pairwise with the other two quarks of the cluster. Occasionally, the cluster mass may be too light to decay isotropically into two hadrons based on kinematic concerns. In this case, it must be combined with a nearby cluster with energy and momentum conservation preserved by an exchange of four-vector.

Since this model reduces the complicated parton shower into manageable quark pairs, it is straight-forward to try to associate final state products with the initial state partons. However, one cannot guarantee that a particular product of a cluster decay can be attributed uniquely to a particular parent quark. This is due to the fact that within a cluster, colour interactions between the quarks will effectively allow energy to flow from one parent to the other thus yielding products that cannot be unambiguously matched with any one of the parent quarks.

## 1.2 Lund String Model

In string fragmentation, the idea is to model the fragmented partons by a massless relativistic one dimensional string with no transverse degrees of freedom. The energy in the various partons are then transferred into the various pieces of the string linking them, effectively giving the string an energy density. The resulting hadrons are formed when the pieces of the string “break,” thus generating the energy necessary for a  $q\bar{q}$  pair to emerge.

In practice, a generic string will be composed of two quarks (or diquarks) on either end with a number of gluons in between. Typically, fragmentation begins at both ends at the same time and ends in the middle at a certain string energy threshold.

A hadron is produced by introducing a  $q_1\bar{q}_1$  pair with randomized flavour for each string piece and combining it with the quark at the end of the string ( $q_0$ ). The hadron ( $q_0\bar{q}_1$ ) will be produced. The procedure can continue by introducing another  $q_2\bar{q}_2$  pair and producing a hadron ( $q_1\bar{q}_2$ ). This process continues until the final string piece is below the specified energy threshold (a parameter in the model) at which time, a final pair of hadrons will be produced.

One can see that the advantage of this model is that the final products can essentially be identified uniquely with one of the end quarks of the string depending on which side it fragmented off of. However there will be some energy flow and thus some ambiguity between the the two ends of the final string that fragments. Colour connections are made by associating all colour connected partons into one string. Colour flow interactions are modelled by the energy exchange among the two ends of the string as well as between the various pieces of the string.

## 2 Procedure

The purpose of this study is to characterize the effect of colour flow between the initial state partons of the collider beam and the  $b$  quark on the final  $b$  jet energy. This study will be carried out at the OBSP level with the  $b$  jet energy characterized by summing the energies of all stable final state OBSP particles that lie within some cone of the  $b$  jet (typically  $R = 0.4$ ). Ideally, we would like to be able to determine exactly how much energy flow has occurred between the beam and the  $b$  quark. However, due to the complexity of the process, we must resort to a more practical measure of this effect.

In the hadronization process, regardless of the model used, a number of particles are produced from the fragmentation of the  $b$  quark. Since the  $b$  quark is colour connected to partons in the initial proton beam, it is reasonable to expect some colour interactions between them. This colour flow yields particles that may not correspond unambiguously to any particular parent parton. As a result, we can attempt to define a measure of “ambiguous” energy attributed specifically to the  $b$  quark. We then characterize the colour flow effect by a measure of the amount of “ambiguous” energy that is deposited within a cone of radius  $R$  of the  $b$  jet. While the notion of “ambiguous” energy is general for any hadronization model, the actual definition will depend considerably on the actual model used. We will describe in detail the definition we use for both the Cluster Hadronization Model (Herwig) and the Lund String Model (PYTHIA) in the following subsections.

## 2.1 HERWIG

In order to characterize “ambiguity” at the OBSP level, it is first of all necessary to establish unambiguous mother daughter links at this level. To do this we must first establish the same type of link at the HEPG level. In HERWIG, for each quark that will undergo fragmentation, a special entry in the HEPG bank is created corresponding to a “jet.” Partons belonging to this jet will be identified by the pointer `jmo1hep` of the HEPG bank. Colour (or anticolour) connections are specified through the `jda2hep` pointer (`jmo2hep`) in the HEPG bank. Those partons which are connected in this way, will be combined into special entries specified by the special cluster particle type. These cluster will then decay into 2 hadrons which then subsequently decay into stable observable particles. In this way, the OBSP particles can be linked uniquely to a particular cluster decay.

The ambiguity lies in the decay of the cluster. It is not clear which quark produces which hadron. In fact, in some cases a unique assignment simply cannot be made. In the case where both partons arise out of the same “jet,” this question is rendered irrelevant because both products will be associated with that parent “jet.” A problem occurs in cases where the constituent quarks of a particular cluster come from different “jets.” In many cases, the cluster decays in such a way that the energy and momentum of the products closely mimic the energy and momentum of the original quarks. There are also cases when one quark contributes negligibly to the cluster. In both cases, we wish to define a procedure by which unique parent daughter assignments can be made between the products and the parent quarks, and subsequently the jets.

### 2.1.1 Defining an Appropriate Mapping Scheme

To motivate a quantitative measure of the “negligibility” of the energy flow within the cluster, we plotted  $\Delta E/E_{parton}$  versus  $E_{parton}$  for each cluster system shown in Fig. 1 with the following precise definitions:

- $E_{parton}$  is the energy of the most energetic quark in a cluster.
- $\Delta E = E_{product} - E_{parton}$ , where  $E_{product}$  is the energy of the hadron produced whose energy is closest to  $E_{parton}$ .

Essentially,  $\Delta E$  is a measure of the amount of energy flow within a cluster. The scatterplot confirms that the energy flow actually scales with the energy of the cluster, so that a more reasonable measure is the ratio  $\Delta E/E_{parton}$ .

The plot not only identifies the correct range of “negligibility” but also shows some asymmetry with respect to  $\Delta E$ . The energy flow seems to favour the parton side, indicating that energy tends to flow more from the higher energy parton to the lower energy parton. We identify the “negligible” region to be  $-0.015 \leq \Delta E/E_{parton} < 0.01$ . We note that these considerations only apply to relatively high energy partons, and in our subsequent analyses will be only considering partons with energies above 10 to 15 GeV. Motivated by this measure of “negligibility” we extend the same definition to the case where the cluster is composed of quarks contributing very small amounts of energy to the cluster. In the case where one quark contributes energy less than 0.01 of the total cluster energy, then both products of the cluster decay will be assigned to the other quark and its “jet.” Preference

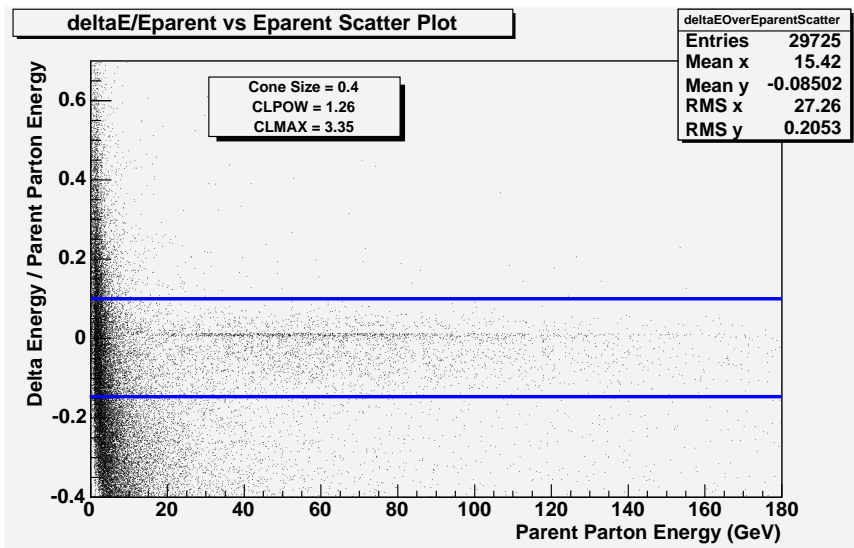


Figure 1: A scatterplot showing the distribution of energy flow with increasing cluster energy.

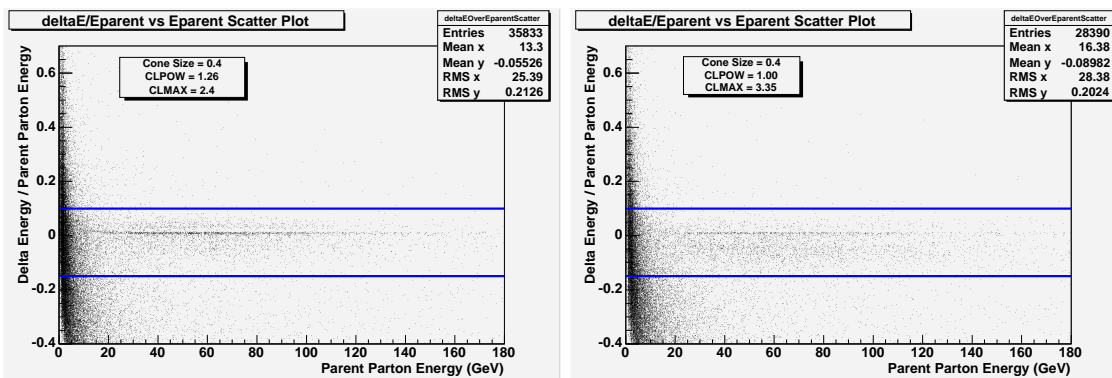


Figure 2: The same scatterplot of the energy flow distribution for varying model parameters in HERWIG.

will be given to the first situation where both cases apply. The rest of the products will be defined to be “ambiguous” daughters.

Figure 2 shows the same distribution for varied model parameters CLMAX and CLPOW. Although there are some differences in the distribution, the plots show that the definition of “negligible” that is used is a reasonable one for any value of these parameters. Those points that are to be identified as negligible still lie well within the limits that we have set.

### 2.1.2 Identifying the $b$ Jet

Having completed the mapping of all  $b$  “jet” daughters, we must now identify the correct jet reconstructed by the JETCLU module. The standard method that is used is to look for the jet whose coordinates (in  $\eta$ - $\phi$  space) is closest to the direction of the original  $b$  quark and establish some maximum separation distance to the  $b$  quark (for example  $R = 0.4$ ). In this

study we use a slightly different algorithm. We assign individual OBSP particles to the jet whose  $\eta - \phi$  coordinates are closest to the particle coordinates, still requiring that  $\Delta R < ??$ . We then iterate through all the jets and identify the jet containing the most  $b$  daughters as the “ $b$  jet.” [5]. Although this method of identifying the appropriate reconstructed jet produces similar results to the standard technique of associating the closest jet in  $\eta - \phi$  space, we have not characterized in detail the differences.

### 2.1.3 Defining the Measure of the Colour Flow Effect

Now having established which particles are “ambiguous” at the OBSP level, we now define the measure of the colour flow effect by the mean of the ratio:  $E_{T\text{ambiguous in jet}}/E_{T\text{total in jet}}$ , where  $E_{T\text{ambiguous in jet}}$  is given by the sum of the  $E_T$  of all stable OBSP particles which lie within some radius  $R$  of the  $b$  jet and that are ambiguous as defined above. In addition, several kinematic cuts are made to conform to more realistic experimental conditions. Only jets whose  $E_T$  is above 15 GeV is considered. We also require that the jets have  $\eta$  between -2.0 and 2.0. Finally, to get a more accurate measure of the colour flow effect, we neglect those events for which no ambiguity at all are found. These events occur about one-third of the time.

Moreover, we will study the dependence of this mean on the size of the jet cone radius  $R$  as well as the scaling of this effect with increasing  $b$  parent quark  $E_T$ . Finally, we will examine the dependence of this effect on the parameters of the cluster hadronization model. Specifically, we study the dependence on the mass threshold for cluster splitting and the two parameters that define it (CLMAX and CLPOW).

## 2.2 PYTHIA

Contrary to Herwig, PYTHIA handles fragmentation by combining all partons of colour connected “jets” into a single string entry with the internal PYTHIA particle code IDHEP = 92. In general, a string consists of two quarks (or diquarks) at either end with a number of radiated gluons in between. A switch - MSTU(16) - in the PYTHIA program allows us to define parent daughter links between the hadrons and the quarks directly. The JMO1HEP pointer of the products will point to one of the original parent quarks depending on the details of the string fragmentation, namely which side of the string the hadron fragmented from. Thus, we have a direct link between the final state OBSP particles and the original quarks.

### 2.2.1 The PYTHIA Mapping Scheme

Since there is a direct link between the daughters and parent quarks in PYTHIA, it is a much easier process to define an assignment scheme. The problem, however, lies in the fact that the final two hadrons produced fragmented from quarks that presumably had a chance to experience energy flow. This means that the final two hadrons may contain some unidentified energy flow. Unfortunately we have not been able to identify these final pairs consistently and thus this assignment actually misses some of the colour flow information in this final step.

Since the  $b$  quark is always colour connected with some partons of the proton beam, it will always be combined with another parton (typically a diquark) from the beam into a single string. We assign those products which fragmented off the  $b$  quark side of the string as  $b$  daughters, and those that fragmented off the other side as ambiguous daughters. This is a reasonable definition considering that we are interested primarily in those products affected by the underlying colour interaction between the  $b$  quark and the beam. A measure of how much of these particles are deposited within the  $b$  jet cone is a reasonable measure of the colour flow effect.

### 2.2.2 Defining the Measure of the Colour Flow Effect

Having obtained the  $b$  daughter mapping, we identify the  $b$  jet in the same way as in HERWIG above. Likewise, we choose to measure the colour flow effect in the same way as before, by measuring the mean of  $E_{T\text{ambiguous } b \text{ jet}}/E_{T\text{total } b \text{ jet}}$ . It is useful to note that this measure is actually not the same as the measure for HERWIG because of the change in our definition of ambiguity. Finally, the same kinematic cuts are applied as for HERWIG.

## 2.3 A General Comparison Between HERWIG and PYTHIA

To relate this study to more general properties of  $b$  jets, we compare some other properties of jets between the two Monte Carlo samples. Specifically, plots of  $E_{T\text{jet}}/E_{T\text{parent}}$  and  $P_{T\text{jet}}/P_{T\text{parent}}$  for both  $b$  jets and  $W$  jets are studied. An alternative definition of  $E_{T\text{jet}}$  is used in this study; it is defined to be the sum of the  $E_T$  of all OBSP particles that lie within some radius  $R$  of the jet, and similarly for  $P_T$ . This definition is used to try to isolate the effect of colour flow and fragmentation on the jet energies and to eliminate other detector and calorimeter based effects. Finally, the energy flow further away from the jet cone is examined by looking at the amount of energy deposited by OBSP particles within the annulus from a radius of 0.4 to 0.6 of the jet.

We note that this definition of jet energy is quite different than the one provided by JETCLU. In the JETCLU case, we would expect to see peaks in the ratio of  $E_{T\text{jet}}/E_{T\text{parent}}$  around 0.7 for  $b$  jets and between 0.7 and 0.8 for  $W$  daughter jets.

## 3 Results

### 3.1 Herwig

From the histograms of  $E_{T\text{ambiguous } b \text{ jet}}/E_{T\text{total } b \text{ jet}}$  shown in Fig. 3, we conclude that the colour flow effect accounts for about 3% of the energy deposited within the  $b$  jet cone of radius 0.4. The dependence of this measure on the jet cone radius is plotted in Fig. 4. One sees that there is a clear peak at around  $R = 0.8$  with a slow fall-off as the radius is increased further. We understand the fall-off at larger  $R$  as resulting from the fact that the added energy from underlying events begins to be larger than the additional ambiguous energy, causing the effect to peak or plateau. It is interesting to note the range of values that this measure takes varies between 2.0% to about 3.3%. It is reasonable to expect that the actual effect lies somewhere in this range.

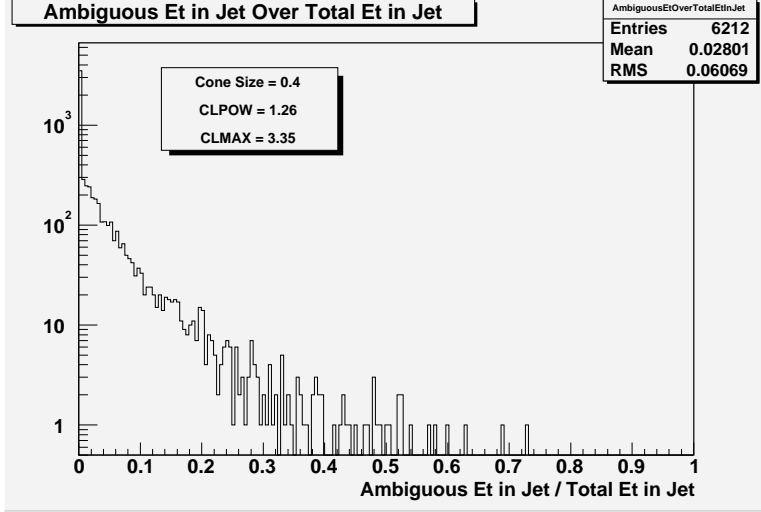


Figure 3: Histogram of the colour flow measure for the  $b$  jet cone of radius 0.4 for the HERWIG sample. A semi-log scale is used for clarity.

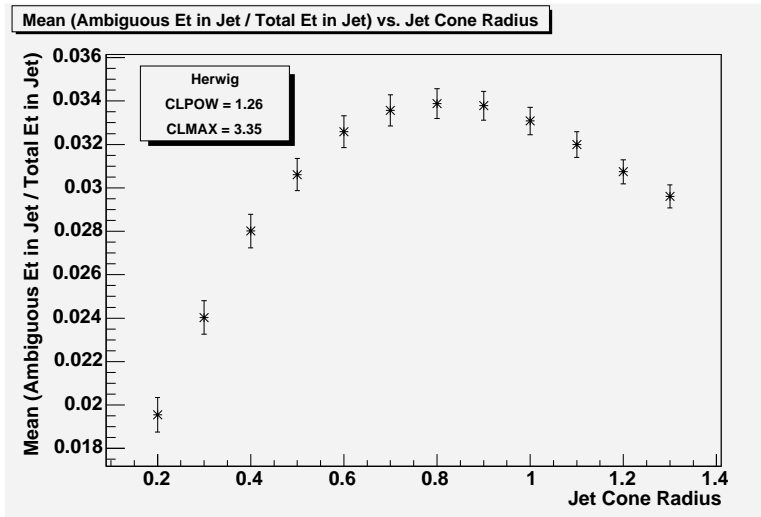


Figure 4: A graph of the mean measure of colour flow vs. Jet cone radius for the HERWIG sample.

Profile plots of this mean value versus  $b$  quark  $E_T$  and  $b$  jet  $E_T$  are shown in Figure 5 and 6, respectively. They both indicate that the raw colour flow effect scales up as the energy of the system is increased. Ignoring the low and high  $E_T$  extremes -these are likely due to a lack of statistics- the mean is more or less constant around the value of 3%.

Figure 7 shows the dependence of the colour flow measure on the HERWIG parameter CLMAX, with CLPOW held constant at the default value of 1.26. The effect steadily decreases from 3.1% to 2.5% as CLMAX is increased from 2.4 GeV to 4.3 GeV. This is a reasonable behaviour since, from the formula for the maximum cluster mass threshold in Eq. (1), one sees that for fixed CLPOW, increasing CLMAX gives essentially an additive effect on the mass threshold. Since for increased mass threshold, less clusters will be forced

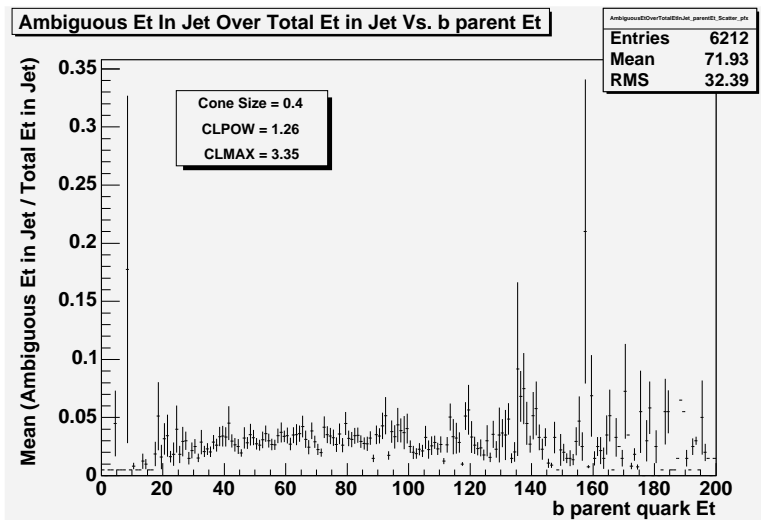


Figure 5: Profile Plot of the mean measure of colour flow vs.  $E_{Tb_{parent}}$  for the HERWIG sample.

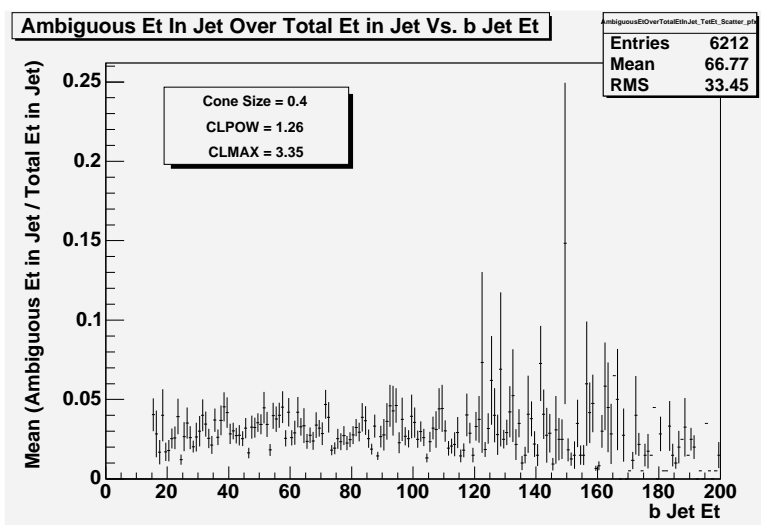


Figure 6: Profile Plot of the mean measure of colour flow vs.  $E_{Tb_{jet}}$  for the HERWIG sample.

to split, we would expect that the colour flow effect will be less pronounced.

The dependence on the parameter CLPOW is shown in Figure 8 with CLMAX held constant at the default value of 3.35 GeV. The effect scales up as CLPOW is increased until it reaches a plateau at CLPOW= 2.4. Again, there is a simple interpretation in terms of the mass threshold formula. Assuming that the constituent quark masses are low compared to the default CLMAX value of 3.35 GeV, a reasonable assumption since most clusters are composed of light quarks, one can expand the formula for the mass threshold in a power series. For increasing CLPOW, higher order terms become negligible and the mass threshold becomes constant. Thus, we would expect that the colour flow effect will plateau for increased CLPOW.

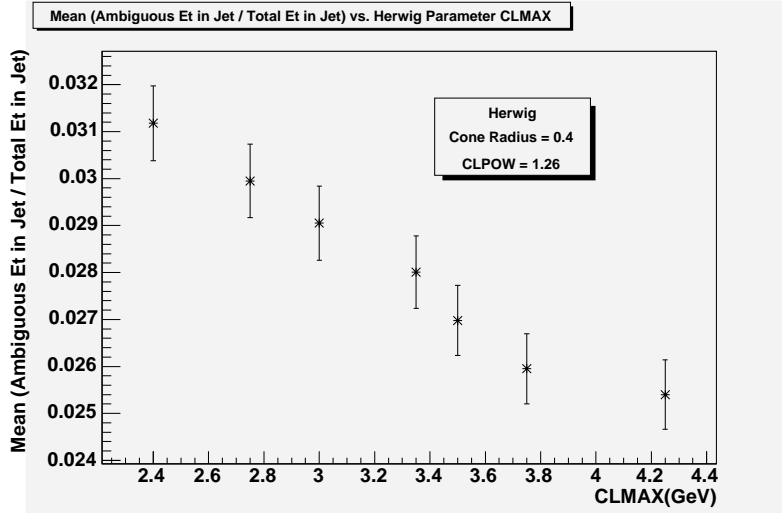


Figure 7: Graph showing the dependence of the mean measure of colour flow versus the HERWIG parameter CLMAX.

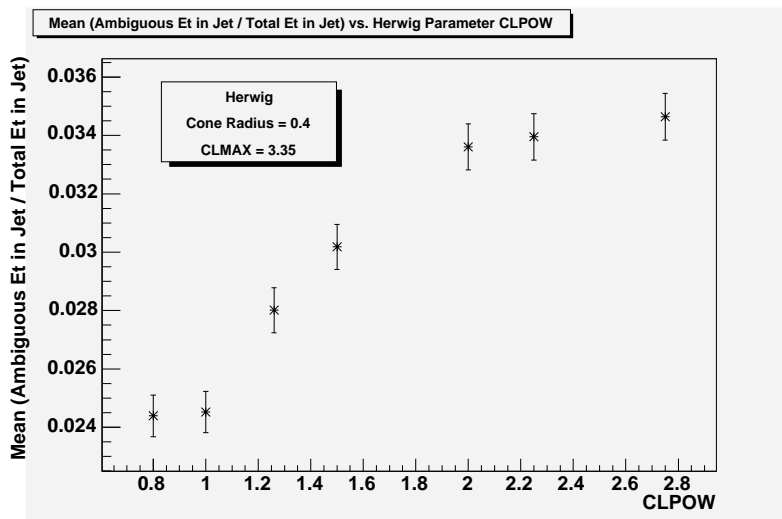


Figure 8: Graph showing the dependence of the mean measure of colour flow versus the HERWIG parameter CLPOW.

In summary, the colour flow effect is very much dependent on the cluster mass threshold. The effect decreases as the cluster mass threshold increases since less cluster splitting will occur. The overall quantitative measure of this effect appears to range from  $\tilde{2}.5\%$  to  $\tilde{3}.5\%$  as different model parameters are used. Again, this supports our conclusion that the real effect lies somewhere around 3%.

### 3.2 PYTHIA

Histograms for the same colour flow measure for PYTHIA is shown in Fig. 9. One sees that the effect is diminished by about a factor of two for PYTHIA; the average effect is about

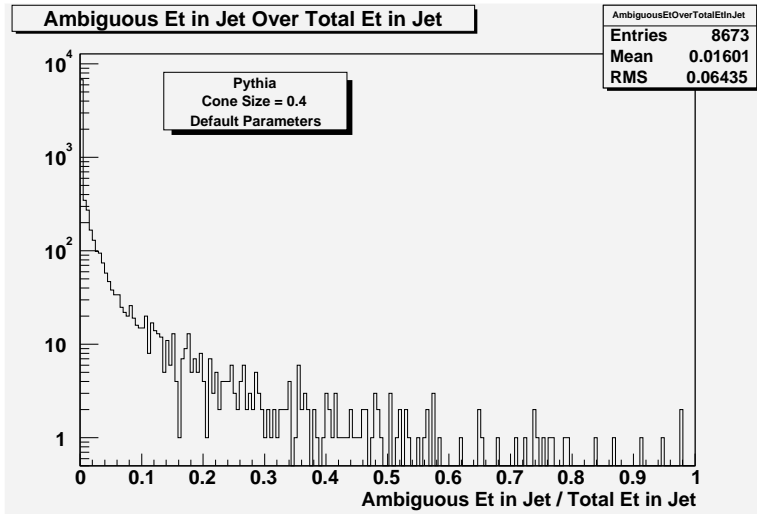


Figure 9: Histogram of the measure of colour flow for a jet cone of radius 0.4 for the PYTHIA sample.

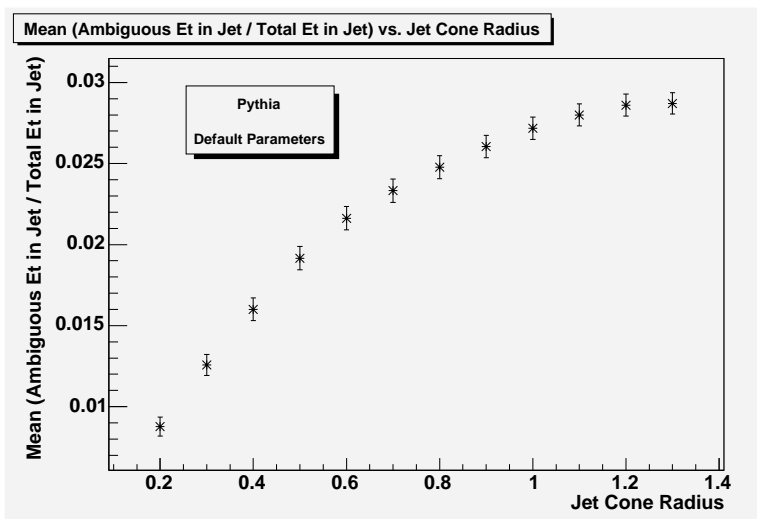


Figure 10: A graph of the mean measure of colour flow vs. Jet cone radius for the PYTHIA sample

1.5%.

The dependence of the colour flow measure on the  $b$  jet cone radius  $R$  is shown in Fig. 10. Again, the colour effects increase as the cone radius is increased; however it does not show the prominent peak that the HERWIG plot displayed. Instead, the effect begins to flatten out at a slightly larger radius at  $R = 1.1$ . This feature is most probably due to different default settings pertaining to underlying events for PYTHIA and HERWIG, and not really a result of differences in colour flow between the two models. The interesting feature to note is that the colour flow measure averages around 2% ranging between 1% and 3%, as the cone size is increased.

The difference is mainly interpreted as a difference in our definition of ambiguous energy.

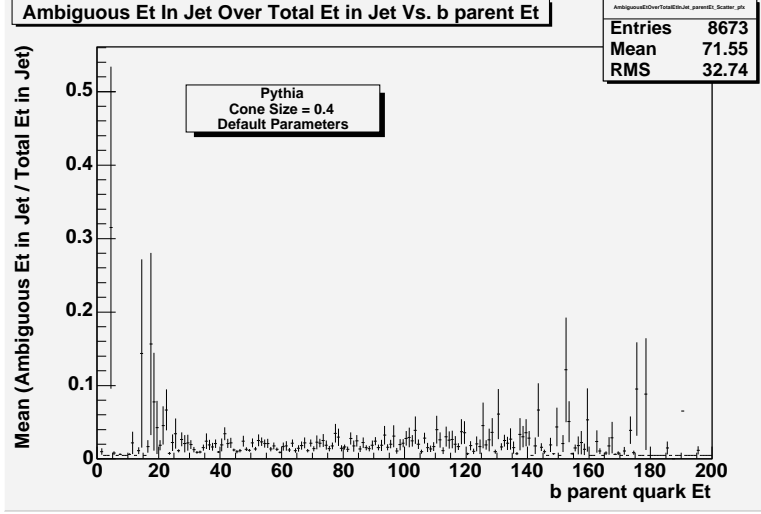


Figure 11: Profile Plot of the mean measure of colour flow vs.  $E_{Tb\ parent}$  for the PYTHIA sample.

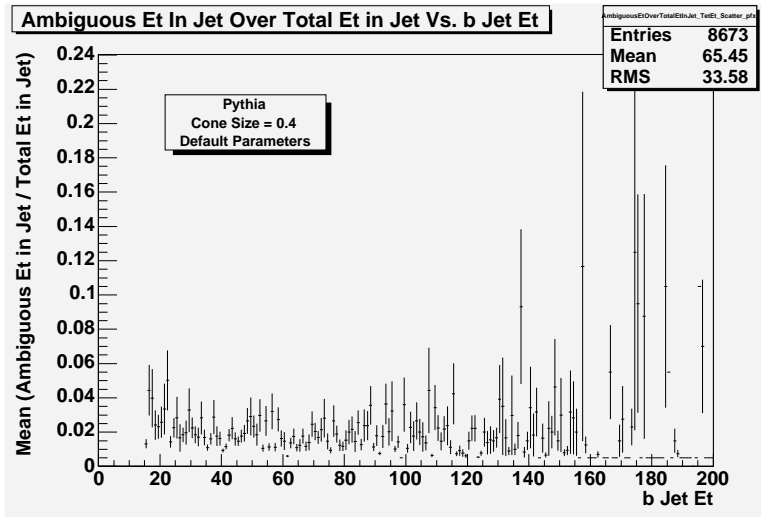


Figure 12: Profile Plot of the mean measure of colour flow vs.  $E_{Tb\ jet}$  for the PYTHIA sample.

In PYTHIA, we failed to account for the energy flow in the last pair of hadrons produces. We hypothesize that this is the main reason for the diminished effect. The conclusion that this measure allows us to draw is that colour interactions between the beam and the  $b$  quark is responsible for depositing about 1.5% of the total jet energy of daughters of the beam partons into a cone of radius 0.4 around the  $b$  jet.

Figures 11 and 12 show the scaling of the effect with the  $b$  quark and  $b$  jet  $E_T$ . Analogous to HERWIG, the plots show that the raw effect scales up with energy. Again, ignoring the extremes the effect is basically constant at around 1.5%.

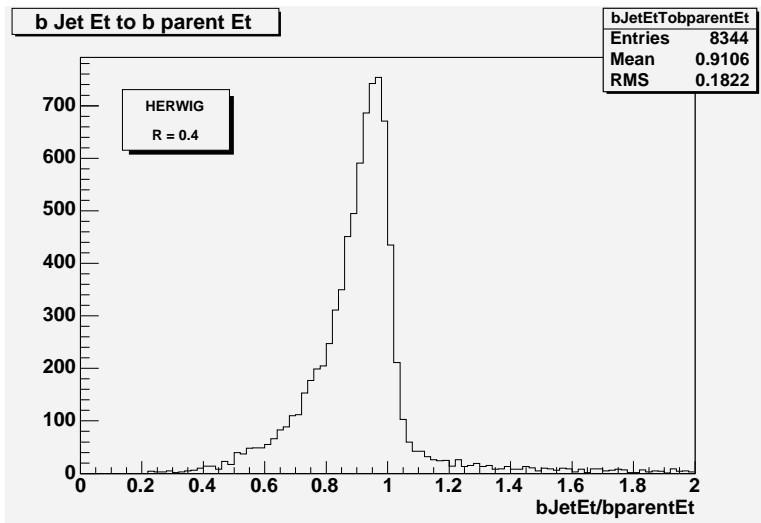


Figure 13: Distribution of  $(E_{Tb\ jet}/E_{Tb\ parent})$  for Herwig

### 3.3 A Comparison of General Jet Properties between Herwig and PYTHIA

Recalling the difference in our definition of jet energy, Figures 13 and 14 show the distribution of  $(E_{Tb\ jet}/E_{Tb\ parent})$  in Herwig and PYTHIA respectively. Similarly Fig. 15 and 16 show the same distribution for the  $W$  jets with  $E_T$  of the two jets summed. Two prominent features are worth noting. The fact that the  $b$  distribution has shifted further away from 1.0 while the  $W$  distribution has not, indicates that some energy flow out of the cone has occurred for the  $b$  jet, presumably from interactions with the beam, whereas no such effect is observed for the  $W$  jets. The second observation is that the shift in the  $b$  distribution is greater for the PYTHIA sample (Let's discuss this with Jean-Francois on Tuesday?). Moreover, no significant difference is observed between PYTHIA and HERWIG for the  $W$  distribution. This supports the conclusion that this difference is at least partly due to colour flow effects since it seems to only affect the  $b$  jet. We also conclude that string fragmentation leads to a greater energy flow between the  $b$  quark and the beam partons. Curiously, this seems to contradict the results of the previous subsection; however recalling that the definition of ambiguity is different in the two models, it is actually not that surprising that PYTHIA is observed to have the larger colour flow effect, particularly since the effect is actually not very large. This apparent contradiction is worth further study, perhaps by defining a better measure of ambiguity in string fragmentation.

Since the  $W$  jet  $E_T$  plot will actually depend on the  $W$  mass, we plot the same distribution for  $P_{Tjet}/P_{Tparent}$ , where  $P_{Tjet}$  is defined to be the  $P_T$  of the four-vector obtained by summing the four-vectors of all stable OBSP particles within a radius of 0.4 of the jet, to obtain a more independent crosscheck. The  $b$  jet distributions are shown in Figure 17 and 18 for PYTHIA and HERWIG, respectively. The analogous  $W$  distributions are shown in Figure 19 and 20. Again, there is a more pronounced shift for the  $b$  distributions with PYTHIA showing a greater effect. This supports the conclusions drawn above. Moreover, a rough quantitative characterization can be obtained by looking at the difference in these two mean values. They indicate that the two models give uncertainties in the colour flow effect of about 2% of the total jet energy.

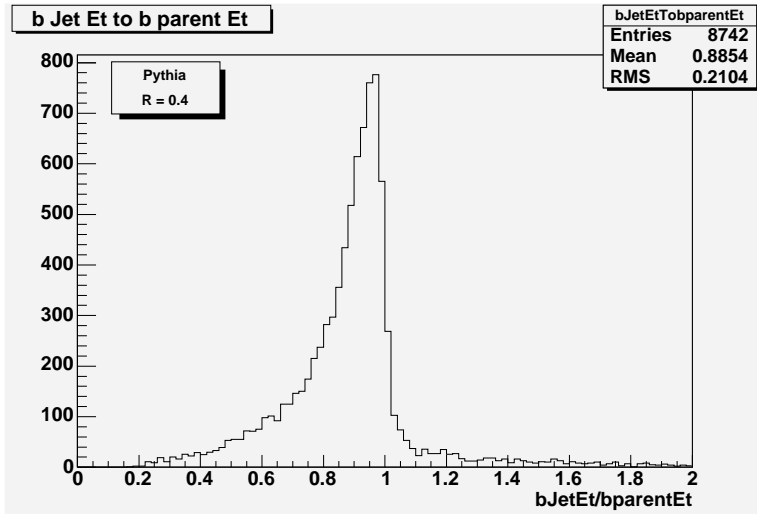


Figure 14: Distribution of  $(E_{Tb\ jet}/E_{Tb\ parent})$  for PYTHIA

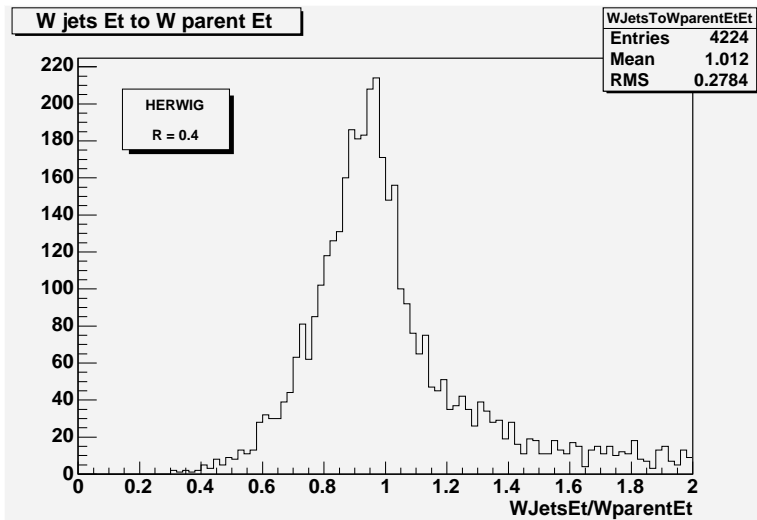


Figure 15: Distribution of  $(E_{TW\ jets}/E_{TW\ parent})$  for Herwig

Generally in top quark physics, one looks at jets with cone radius  $R = 0.4$ . It is perhaps useful to see the energy flow in the region slightly outside of this cone. Figures 21 and 22 show the energy deposited into the annulus of radius 0.4 and 0.6 around the  $b$  jet (at the OBSP level) of the HERWIG and PYTHIA samples, respectively. The same distribution for  $W$  daughter quark jets in Figs. 23 and 24. These show that the behaviour when we extend the jet cone beyond a radius of 0.4 is more or less the same for both models. The effect is slightly greater for  $W$  jets, but the significance of this fact is not so clear since the  $b$  jets in general have much higher energies than the  $W$  jets.

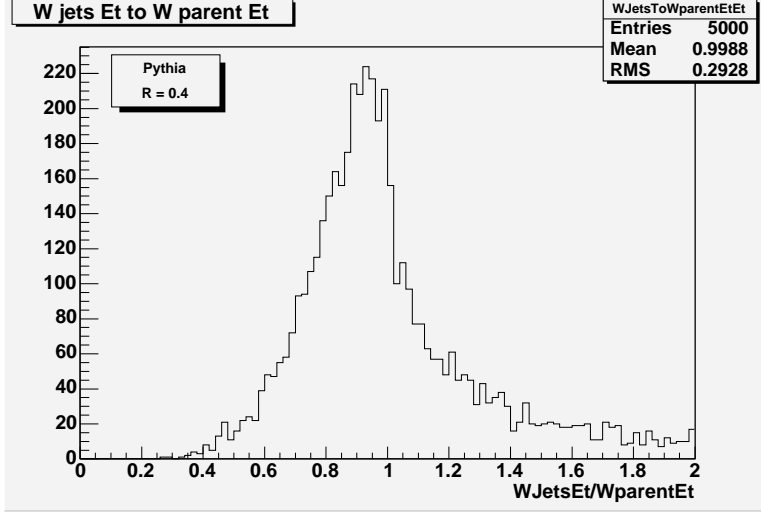


Figure 16: Distribution of  $(E_{TW \text{ jets}}/E_{TW \text{ parent}})$  for PYTHIA

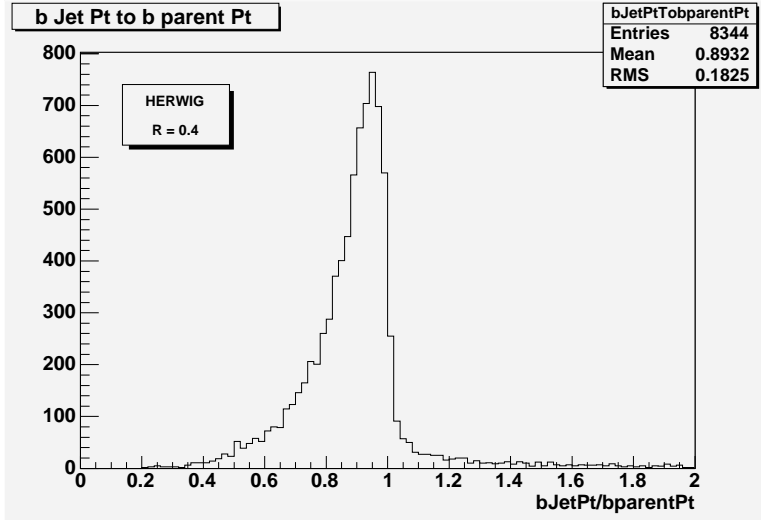


Figure 17: Distribution of  $(P_{Tb \text{ jet}}/P_{Tb \text{ parent}})$  for Herwig

## 4 Conclusions

To summarize, the effects of colour flow and fragmentation of the jet energy scale is of great importance for setting better limits on the uncertainties in future top quark mass measurement. The colour flow between the incoming partons and the final state is only an issue for the  $b$  jet, and this study allows us to estimate the jet energy corrections that arise from the colour flow effects and their uncertainties.

We draw several conclusions from this study:

1. The contribution of energy arising from colour interactions with the proton beam to the  $b$  jet is found to be of order 3% of the total  $b$  jet energy.
2. Varying jet cone radii and hadronization model parameters allows us to conclude that

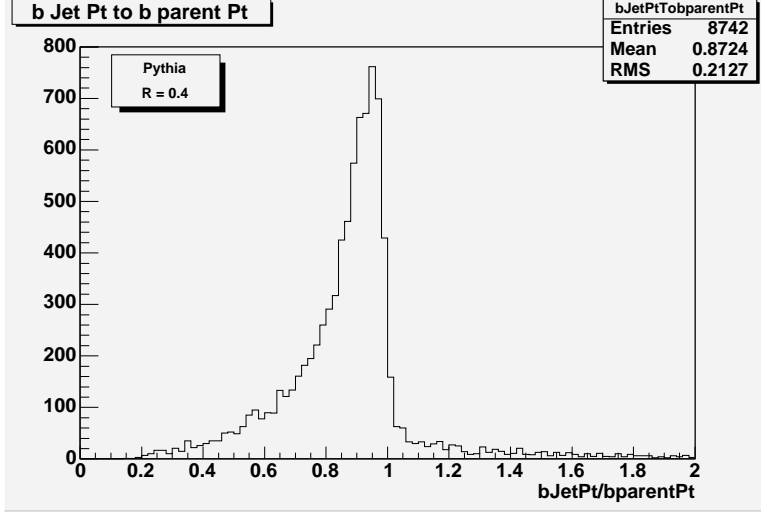


Figure 18: Distribution of  $(P_{Tb\ jet}/P_{Tb\ parent})$  for PYTHIA

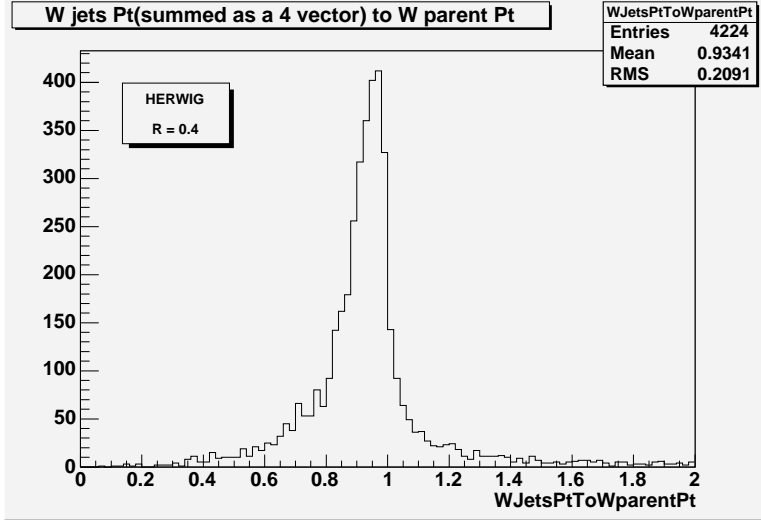


Figure 19: Distribution of  $(P_{TW\ jets}/P_{TW\ parent})$  for Herwig

the modelling of the fragmentation models create systematic uncertainties that are not larger than 1% of the b jet energy scale.

3. Differences in overall fragmentation and decay models employed by HERWIG and PYTHIA suggest that the relative modelling of b jets and  $W$  daughter jets have a systematic uncertainty of perhaps 1% of the b jet energy scale (we should discuss this further).

We note that our studies suggest that PYTHIA produces larger colour flow effects compared with HERWIG. This may not seem so unreasonable considering the fact that the string fragmentation mechanism involves many partons whereas the cluster decay involves only two. This is one area of further study.

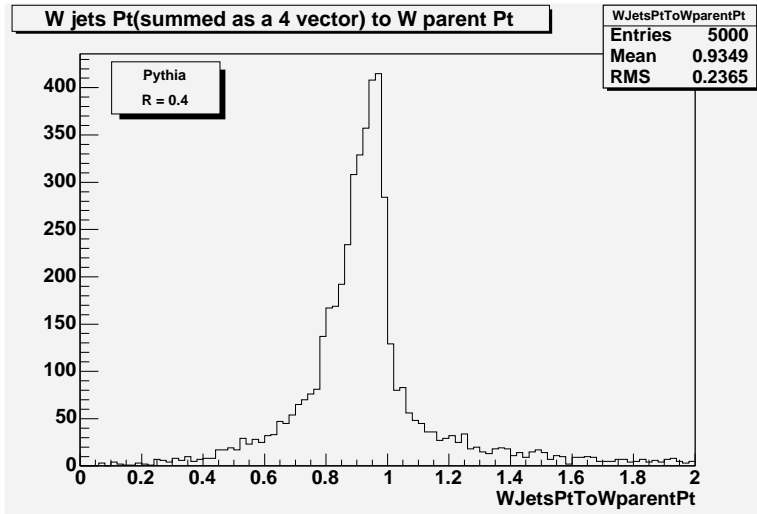


Figure 20: Distribution of  $(P_{TW \text{ jets}}/P_{TW \text{ parent}})$  for PYTHIA

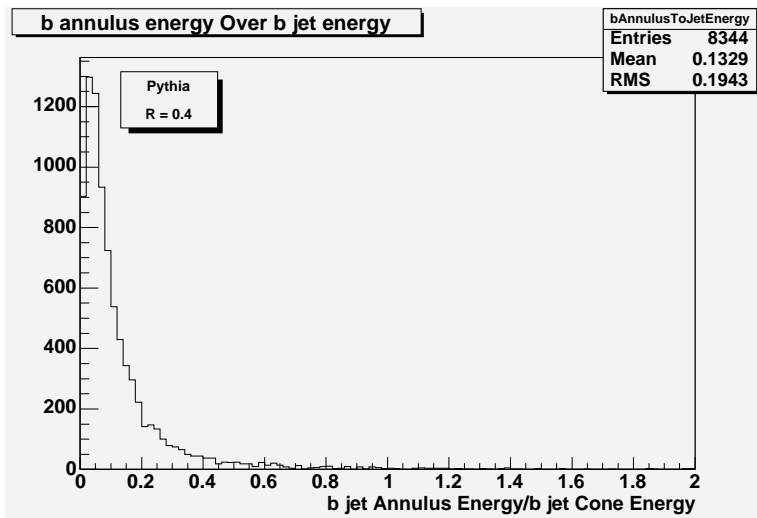


Figure 21: The energy deposited within an annulus of radius 0.4 and 0.6 centered on the b jet cone in the HERWIG Monte Carlo events.

## References

- [1]
- [2]
- [3]
- [4]
- [5] I. Blumenfeld, Fourth-year Engineering Science thesis (April 2004).

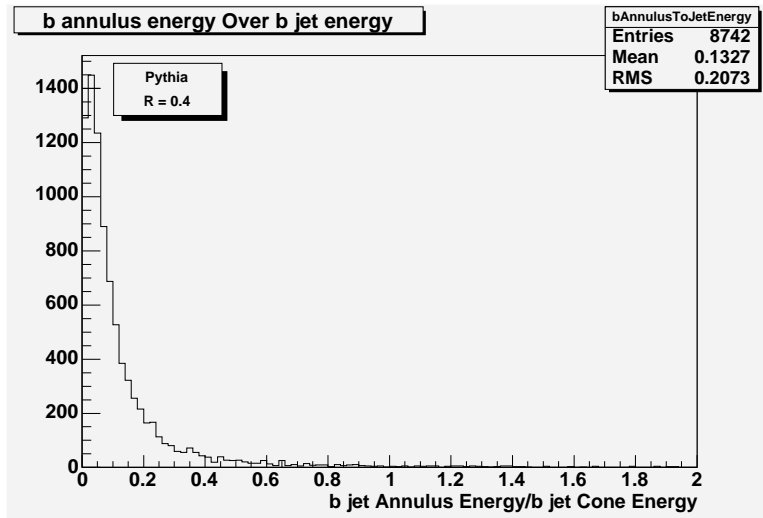


Figure 22: The energy deposited within an annulus of radius 0.4 and 0.6 centred on the b jet cone in PYTHIA Monte Carlo events.

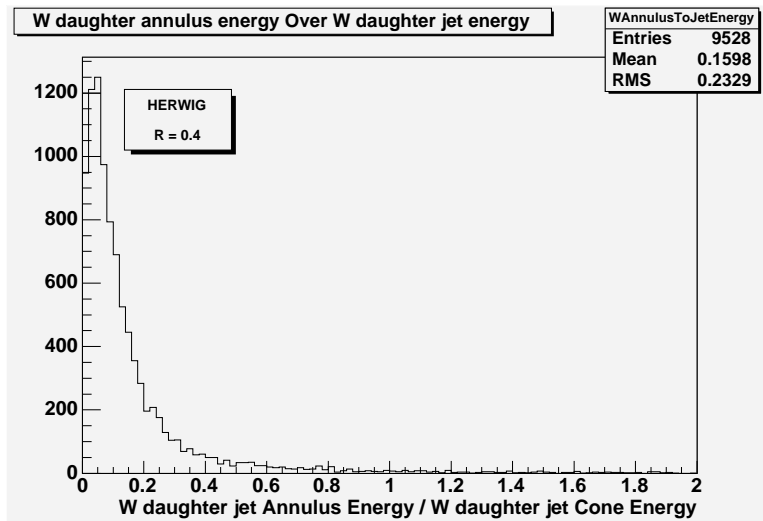


Figure 23: The energy deposited within an annulus of radius 0.4 and 0.6 centered on the W daughter jet cones in HERWIG Monte Carlo events.

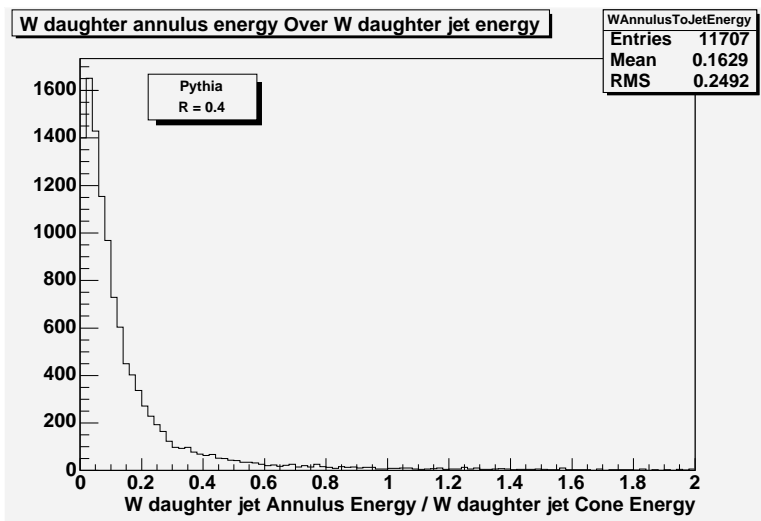


Figure 24: The energy deposited within an annulus of radius 0.4 and 0.6 centred on the W daughter jet cones in PYTHIA Monte Carlo events.